Journal Pre-proof

Treatment of effluents containing 2-chlorophenol by adsorption onto chemically and physically activated biochars

Lauren M.M. Machado (Conceptualization) (Investigation) (Resources) (Writing - original draft), Sabrina F. Lütke (Methodology) (Resources) (Writing - original draft), Daniele Perondi (Conceptualization) (Methodology) (Formal analysis) (Writing - original draft) (Visualization), Marcelo Godinho (Supervision) (Project administration) (Funding acquisition) (Conceptualization) (Writing - review and editing), Marcos L.S. Oliveira (Conceptualization) (Writing - review and editing), Gabriela C. Collazzo (Conceptualization) (Methodology), Guilherme L. Dotto (Supervision) (Project administration) (Funding acquisition) (Conceptualization) (Writing - review and editing)

PII: S2213-3437(20)30822-8

DOI: https://doi.org/10.1016/j.jece.2020.104473

Reference: JECE 104473

To appear in: *Journal of Environmental Chemical Engineering*

Received Date: 1 July 2020

Revised Date: 10 August 2020

Accepted Date: 9 September 2020

Please cite this article as: Machado LMM, Lütke SF, Perondi D, Godinho M, Oliveira MLS, Collazzo GC, Dotto GL, Treatment of effluents containing 2-chlorophenol by adsorption onto chemically and physically activated biochars, *Journal of Environmental Chemical Engineering* (2020), doi: https://doi.org/10.1016/j.jece.2020.104473

Treatment of effluents containing 2-chlorophenol by adsorption onto chemically and physically activated biochars

Lauren M. M. Machado[a], Sabrina F. Lütke[a], Daniele Perondi[b], Marcelo Godinho[b], Marcos L. S. Oliveira[c,d]*, Gabriela C. Collazzo[a], Guilherme L. Dotto[a]**

[a]Chemical Engineering Department, Federal University of Santa Maria - UFSM, Santa Maria, RS, Brazil.

[b]Engineering of Processes and Technologies Postgraduate Program, University of Caxias do Sul - UCS, Caxias do Sul, RS, Brazil.

[c]Department of Civil and Environmental, Universidad De La Costa, Calle 58 #55-66, 080002, Barranquilla, Atlántico, Colombia.

[d]Faculdade Meridional IMED, 304-Passo Fundo, RS, 99070-220, Brazil.

Lauren Marcilene Maciel Machado E-mail adress: lauren_machado@hotmail.com

Sabrina Frantz Lütke E-mail adress: sabrina_lutke@yahoo.com.br

Daniele Perondi E-mail adress: dani.perondi@gmail.com

Marcelo Godinho E-mail adress: mgodinho@ucs.br

Marcos L. S. Oliveira E-mail adress: msilva@cuc.edu.co

Gabriela Carvalho Collazzo E-mail adress: gabriela.collazzo@ufsm.br

Guilherme Luiz Dotto E-mail adress: guilherme_dotto@yahoo.com.br

*Corresponding author: Department of Civil and Environmental, Universidad De La Costa, Colombia. Email: msilva@cuc.edu.co

**Corresponding author: Chemical Engineering Department, Federal University of Santa Maria-UFSM, Brazil. E-mail: guilherme_dotto@yahoo.com.br

Highlights

- Biochars were produced from malt bagasse by activation with CO_2 and $ZnCl_2$;
- The materials were used to treat effluents containing 2-chlorophenol;
- Biochars presented surface areas of 161 $m^2\ g^{-1}$ (CO_2) and 545 $m^2\ g^{-1}$ ($ZnCl_2$);
- $ZnCl_2$-biochar exhibited an efficiency of 98% in the treatment of effluents.

Abstract

The application of adsorption using biochars for the remediation of effluents containing emerging contaminants, including chlorophenols, is a hotspot and trend development in the literature. This treatment is more interesting when using readily available wastes and at no cost, such as malt bagasse, for example. Here, the biochars were produced from malt bagasse, by physical and chemical activation (with CO_2 and $ZnCl_2$, respectively) and employed as adsorbents in the remediation of effluents containing 2-chlorophenol. Results revealed that the activated biochars have mesoporous structures and surface areas of 161 $m^2\ g^{-1}$ (CO_2) and 545 $m^2\ g^{-1}$ ($ZnCl_2$). For both activated biochars, adsorption of 2-chlorophenol was favored under acid conditions, with the highest adsorption capacities found using $ZnCl_2$-activated biochar. The maximum adsorption capacity using $ZnCl_2$-activated biochar was 150 mg g^{-1}. The process was endothermic and spontaneous. $ZnCl_2$-activated biochar exhibited an efficiency of 98% (using a dosage of 10 g L^{-1}) in the treatment of industrial effluents containing 2-chlorophenol.

Keywords: 2-chlorophenol; adsorption; biochar; malt bagasse; pyrolysis.

1. Introduction

Aromatic organic compounds, such as chlorophenols (CPs), are an essential group of emerging contaminants (ECs), extremely difficult to biodegrade [1]. Since they are high toxicity components, carcinogenic and mutagenic, CPs are priority and hazardous contaminants [2]. CPs are widely used in industrial applications, manufacturing herbicides [3], insecticides, pesticides, wood preservation, and as a result, are commonly found dispersed in aquatic resources, soil, and industrial effluents [4]. Based on the environmental risks caused by CPs, its removal from effluents is required. The removal of chlorophenols from effluents can be performed by chemical, biological, and physicochemical treatments [5]. On the one hand, some of these techniques have complex processes, high energy consumption, low removability, the addition of chemical agents, thus increasing the cost of the process involved. On the other hand, the adsorption technique presents high efficiency, simplicity in the application process, resulting in a low operation cost [6]. In the adsorption process, contaminants present in aqueous solution are transferred to a solid (adsorbent) phase [7,8]. Subsequently, the adsorbent can be regenerated [7,9] or stored in a moisture-free place and, the polished effluents can be released or reused in processes that do not require high purity water [7].

Activated carbon is commonly employed as an adsorbent for contaminants removal from liquid streams. This material has high pore volume and upper surface area, favoring the efficiency of the adsorption process. However, the use of this material on a large scale becomes expensive [5]. As a result, biochars derived from no-cost alternative wastes, and prepared by alternative routes have gained attention [9] to make the adsorption process more attractive. In this context, malt bagasse (a by-product

resulting from the malt germination process in the brewing industry) is inserted. This biomass represents 85% of the waste generated in the brewing industry [10]. The production of 100 liters of beer generates approximately 20 kg of malt bagasse [11]. The biochar produced from this biomass can be activated chemically, physically, or by combining them, providing the enrichment of the material characteristics [12].

Concerning chemical activation, various chemicals, like H_3PO_4, $ZnCl_2$, K_2CO_3, KOH, $CaCl_2$, Na_2SO_4, H_2SO_4, have been used [13]. $ZnCl_2$ stands out because it tends to improve the pore development in the biochar structure, providing a high carbon yield [14]. In a complementary way, physical activation by CO_2 is used. Other reagents, including oxygen, steam, and air, can be used for physical activation. However, CO_2 leads to a better development of microporosity [15].

The scientific contribution of this work is the preparation of biochars activated with $ZnCl_2$ and CO_2, using malt bagasse as a precursor and the subsequent application of these biochars as efficient materials to treat effluents containing 2-chlorophenol. The materials were carefully characterized and, the adsorptive potential was analyzed in relation to the activation techniques. A standard adsorption study in synthetic solutions (only 2-chlorophenol) involving kinetic, equilibrium, and thermodynamic was carried out. Additionally, regeneration experiments and simulations with a real effluent were performed.

2. Materials and methods

2.1. Materials

The biomass employed for the development of activated biochars was barley malt bagasse, which was furnished by a beer industry, located in southern Brazil. The biomass was naturally dried in the sun for 48 h, followed by oven drying at 50 °C for 6 h, and milled to generate a material with particle size smaller than 0.5 mm.

For the adsorption experiments, 2-chlorophenol solution (128.56 g mol^{-1} and 99% purity) was supplied by Sigma-Aldrich. For chemical activation, CaO (56.08 g mol^{-1}, 95% purity) and $ZnCl_2$ (136.30 g mol^{-1}, 97% purity) were obtained from Dinamica (Brazil). CO_2 (purity 95%) was supplied by White Martins (Brazil).

2.2. Preparation of biochar adsorbents

During the development of this work, three materials were prepared, characterized, and used for adsorption purposes (biochar and two activated biochars).

The first material produced (biochar without activation) was pyrolyzed from an initial investigation of different operational parameters of temperature and holding time. For this, the following temperatures were investigated: 500, 600, and 700 ºC. Besides, the following holding times were evaluated: 10, 30, and 50 min. The characteristics of the different biochars produced were presented in a recent publication by our group [16]. Through these preliminary results, an optimal experimental condition was obtained (isotherm time of 10 min and a temperature of 500 °C). This condition was then adopted for this work.

The biochars activation procedure was subsequently conducted. The methods adopted for biochar activation with $ZnCl_2$ and CO_2, as well as the parameters evaluated in the adsorption experiments, are presented in Fig. 1.

The methodology used for biochar activation with $ZnCl_2$ was conducted, according to Streit et al. [17]. The procedures adopted are presented in Fig. 1, including the pyrolysis and chemical activation step. In a simplified way, the procedure involves preparing a precursor by mixing CaO (10 % wt.), $ZnCl_2$ (40 % wt.), distilled water, and 40 g of malt bagasse. This mixture was conducted under agitation for one hour and then dried at a temperature of 353 K for 24 h. The precursor was finally inserted in the reactor to be pyrolyzed under the following conditions: final temperature (900 ºC), heating rate (5 ºC min^{-1}), holding time (50 min), and nitrogen flow rate of 150 mL min^{-1}. The reactor used was previously described by Zazycki et al. [9]. The final step to obtain activated biochar was the leaching with HCl 6 mol L^{-1} for 24 h in an orbital shaker (with a ratio of 10 mL HCl:g $material^{-1}$), to remove Zn, and subsequently, washing procedure with deionized water until the neutral pH solution. The material was dried in an oven for 12 h at 50 °C.

For CO_2 physical activation, the biochar was initially prepared by pyrolysis with N_2 (500 °C and 10 min). Subsequently, N_2 flow was replaced by CO_2. The biochar was activated until 900 °C and remained at this temperature for 50 min. The detail of the activation process was reported in another work [11].

2.3. Characterization of activated biochars

$ZnCl_2$ and CO_2 activated biochars were characterized by different techniques as follows: scanning electronic microscopy (SEM), Fourier transform infrared spectroscopy (FT-IR), specific surface area (BET), pore distribution by BJH (Barret-Joyner-Halenda), X-ray diffraction (XRD) and zero charge point (pH_{PZC}). The characteristics of morphology, functional groups, structure, pore properties, and their

distribution, load potential as (H^+ and OH^-), and surface charge were evaluated. More details of the characterizations used in the materials are presented in the supplementary material (Table 1S).

2.4. 2-chlorophenol adsorption experiments

All tests were conducted in a thermostatic stirrer (Solab, Brazil) at 150 rpm, using 0.01 g of adsorbent and 20 mL of 2-chlorophenol aqueous solution (the vessels with solutions were closed to avoid volatilization of the adsorbate). The adsorption experiments were divided into three steps: evaluation of pH effect and biochar type (biochar, CO_2 activated biochar, $ZnCl_2$ activated biochar), kinetic study and, equilibrium isotherms.

The tests to evaluate the impact of pH and adsorbent type were performed using the three adsorbents produced (biochar, CO_2 activated biochar, $ZnCl_2$ activated biochar). The initial concentration of 2-chlorophenol was 50 mg L^{-1}, 120 min of contact time, and pH from 2 to 12. The pH was adjusted by NaOH and HCl solutions;

Kinetic studies were conducted with 2-chlorophenol solutions at pH 6 and initial concentrations of 25, 50, 100, 200, and 300 mg L^{-1}. Sample collection time ranged from 0 to 120 min;

For isotherm experiments, the different concentrations used for the kinetics were used, submitting them at temperatures of 298, 308, 318, and 328 K. Stirring was carried out until equilibrium.

After all experiments, the remaining 2-chlorophenol concentration in the liquid was determined using a Shimadzu UVmini-1240 UV-VIS spectrometer at 273 nm. All experiments were replicated (n=3), and blank tests were carried out. Adsorption

capacity along the time (q_t) and equilibrium adsorption capacity (q_e) were determined by Eqs. (1) and (2), respectively:

$$q_t = \frac{V\,(C_0 - C_t)}{m} \quad (1)$$

$$q_e = \frac{V\,(C_0 - C_e)}{m} \quad (2)$$

Where, V is the volume of solution (L), m is the mass of adsorbent (g), C_0 is the initial concentration of 2-chlorophenol in the liquid phase, C_t is the concentration of 2-chlorophenol in the liquid phase at each time and C_e is an equilibrium concentration of 2-chlorophenol in the liquid phase, (concentration in (mg L^{-1})).

The concentration levels used in the 2-chlorophenol adsorption were based in the literature. Studies of 2-chlorophenol adsorption on *Adenopus breviflorus* [1] and porous carbon [2] used concentrations until 400 and 100 mg L^{-1}, respectively

2.5. 2-chlorophenol adsorption modeling

The adsorption kinetic data of 2-chlorophenol were adjusted with the pseudo-first order, pseudo-second order, and Avrami models [7, 18]. Langmuir [19] and Freundlich [7] models were fitted to the experimental data to verify the behavior of equilibrium isotherms. The initial sorption rate was also calculated [20].

Thermodynamics was evaluated according to the literature [19, 20]. Values of ΔG^0 Gibbs free energy change (kJ mol^{-1}), ΔH^0 enthalpy change (kJ mol^{-1}), and ΔS^0 entropy change (kJ mol^{-1} K^{-1}) were calculated. The equations used are presented in the supplementary material (Table 2S).

The statistical indicators used to prove the fit quality are presented in the supplementary material (S.3).

2.6. Desorption and reuse tests

Adsorption/desorption cycles were conducted to verify the possibility of reusing the $ZnCl_2$ activated biochar. Adsorption was performed using 200 mL of a 50 mg L^{-1} 2-chlorophenol solution, which was mixed with 0.1 g of adsorbent and stirred at 150 rpm (Solab, SL 222, Brazil) for 120 min and 298 K. The adsorbent was then separated from the liquid phase. Subsequently, the loaded adsorbent was submitted to thermal desorption in an oven for 240 min at 373 K. This process was performed for ten cycles. Thermal desorption was selected due to the volatile character of 2-chlorophenol.

2.7. Treatment of effluents containing 2-chlorophenol

A real effluent was simulated to verify the efficiency of $ZnCl_2$-activated biochar for the treatment of a mixture of aromatics in a medium with high salt concentration. The compounds used are generally found in industrial effluents, specifically from the petrochemical area. The simulated effluent composition is listed in Table 1.

The experiments were conducted using adsorbent dosages of 1, 5, and 10 g L^{-1}. The adsorbent was contacted with 200 mL of the effluent, which was agitated for 2 h at 150 rpm and 298 K. The treatment efficiency was evaluated by acquiring spectra of the simulated effluent before and after the treatments, in the range 200-600 nm, using UV-Vis spectroscopy (Shimadzu, UVmini-1240, Japan).

3. Results and discussion

3.1. Characterization of activated biochars

N_2 adsorption/desorption isotherms and pore distribution by BJH (Barret-Joyner-Halenda) desorption method of both activated biochars are depicted in Fig. 2. It was found that the isotherms are very similar, being of type IV accompanied by hysteresis [23]. Although isotherms are the same type (IV for the two adsorbents), the hysteresis is different (type H3 for $ZnCl_2$-activated biochar and type H4 for CO_2-activated biochar). The pore size distribution for both samples indicated the presence of mesopores. The specific surface area (BET) presented values close to 545 $m^2\ g^{-1}$ and 161 $m^2\ g^{-1}$ for $ZnCl_2$-activated biochar and CO_2-activated biochar, respectively. These values were extremely higher in relation to the biochar without activation (6.5 $m^2\ g^{-1}$), and confirm that the activation efficiently performed. Therefore, the improvement of the structural characteristics of the material was achieved. The $ZnCl_2$-activated biochar sample presented a high area value when compared to the CO_2-activated biochar. This trend corroborates that the textural properties were improved after HCl leaching. According to Streit et al. [17], this occurs as a result of the removal of $ZnCl_2$ and CaO, which were initially added. In summary, both materials were mesoporous and presented interesting values of surface area. However, $ZnCl_2$-activated biochar presented superior characteristics than CO_2-activated biochar.

The XRD patterns of both activated biochars produced are shown in Fig. 2 (c). The diffractograms present a broad peak at approximately $2\theta = 23^{\circ}$, corresponding to the plane (002), which is a feature of amorphous carbon. In general, an amorphous

structure is suitable for adsorption since an amorphous material has more empty spaces that allow the accommodation of the adsorbate molecules.

The FT-IR spectra presented in Fig. 2 (d) was obtained to identify the main functional groups in the activated biochars. It was possible to observe that both activated biochars presented the same bands at 3454, 1635, and 1091 cm^{-1}. The band at 3454 cm^{-1} is due to the stretching of O-H bonds of hydroxyl groups. This band is less pronounced in the CO_2-activated biochar spectrum when compared with the $ZnCl_2$-activated biochar spectrum. The band at 1635 cm^{-1} is related to the C=C stretching bond of the aromatic rings resulting from the dehydration and cyclization of carbohydrates during the pyrolysis process. The band at 1091 cm^{-1} can be ascribed to the C–O stretching of carboxyl groups and bending vibration band of hydroxyl groups [24]. It was also possible to observe that the bands at 2959 and 2855 cm^{-1} are present only in the CO_2 biochar spectrum. These two bands are related to sp^3 C-H stretching of the lignin structure, suggesting that lignin was not completely decomposed. This observation suggests that $ZnCl_2$ activation leads to higher decomposition of the precursor material. Indeed, $ZnCl_2$ can react with the lignocellulosic components increasing the aromatic condensation reactions. $ZnCl_2$ assists the evolution of H_2 from the hydroaromatic structure of the precursor material, leaving the sites on the adjacent molecules, which will undergo aromatization.

Fig. 2 (e) and (f) show the scanning electron microscopy images of $ZnCl_2$-activated biochar and CO_2-activated biochar, respectively, with a magnification of 5000 times. The morphological characteristics of the samples are different. It can be observed that the $ZnCl_2$-activated biochar surface is full of cavities of various shapes and sizes, indicating the generation of abundant porosity in the adsorbent material produced, while the CO_2-biochar surface has some roughness and spherical granules and has much fewer

cavities. These observations can be justified due to the different effects caused by $ZnCl_2$ and CO_2 in the activation step. On the one hand, in chemical activation, the electrolytic effect of $ZnCl_2$ causes the breakdown of side bonds of the cellulose molecules, increasing the inter- and intramicelle spaces and expansion of the cellulose structure. These interspaces present between the carbon layers are responsible for the high porosity of the activated biochar produced [25]. Besides that, $ZnCl_2$ impregnated in the precursor prevents the shrinkage of the particle during the pyrolysis [8]. On the contrary, in physical activation, carbon dioxide acts as an oxidant agent, which reacts with the decomposition products formed in the pyrolysis. Thus, the pores of the biochar are unobstructed, improving the porosity of the material [26]. In this way, CO_2 activation does not lead to the formation of new pores. The SEM results corroborate the textural properties previously described, where CO_2-activated biochar has a lower surface area and lower total pore volume.

The characterization techniques like BET/BJH, XRD, FT-IR and SEM, revealed that the activation with $ZnCl_2$ was more consistent than the activation with CO_2, generating a biochar with a well-developed porous structure, higher pore volume and surface area. This behavior is an indication that the material prepared by chemical activation with $ZnCl_2$ will have a better adsorption potential.

3.2. Effects of pH and adsorbent type on 2-chlorophenol adsorption

The pH of the solution affects the adsorbate molecules and, consequently, affects the adsorption capacity. The surface charge of the adsorbent also depends on the pH. The pH value in which the adsorbent surface charge is zero is defined as the point of zero charge (pH_{PZC}) [27]. When the pH of the solution is lower than pH_{PZC}, the

functional groups of the adsorbent surface are protonated. In this way, the adsorbent surface charge becomes positive. On the contrary, if the pH of the solution is higher than the pH_{PZC}, some surface functional groups of the adsorbent release H^+, and the adsorbent surface acquires negative charge [28]. In this way, when $pH<pH_{PZC}$, adsorption of anionic species is favored, whereas, when $pH>pH_{PZC}$, adsorption of cationic species is favored [29].

pH_{PZC} can be determined by the plot of $pH_{initial} \times pH_{final}$ plot. Fig. 3 (a) shows the $pH_{initial} \times pH_{final}$ plot of the biochars developed in this work. It can be observed that the pH_{PZC} values were 6.28, 3.36, and 6.42 for the non-activated biochar, $ZnCl_2$-activated biochar, and CO_2-activated biochar, respectively. Adsorbents with more acidic surface groups and few basic surface groups present lower pH_{PZC} [30]. Indeed, from the FTIR analysis Fig. 2 (d), it is possible to see that the band assigned to stretching of O-H of hydroxyl groups is more pronounced in the $ZnCl_2$-activated biochar spectrum, indicating that this adsorbent material has more acidic hydroxyls groups on the surface.

The effect of the initial pH on 2-chlorophenol adsorption was investigated by varying the pH from 2 to 12. Fig. 3 (b) report the effect of initial pH using the non-activated biochar, $ZnCl_2$-activated biochar, and CO_2-activated biochar. Firstly, it is possible to observe that the higher adsorption capacities were achieved by the $ZnCl_2$-activated biochar. This behavior can be explained due to the textural properties exhibited by the adsorbents produced. As discussed in the previous section, the activation step provided an increase in specific surface area and total pores volume, respectively, from 6.51 $m^2\ g^{-1}$ and 0.009 $cm^3\ g^{-1}$ (non-activated biochar) to 161.70 $m^2\ g^{-1}$ and 0.039 $cm^3\ g^{-1}$ (CO_2-activated biochar) and to 545.05 $m^2\ g^{-1}$ and 0.109 $cm^3\ g^{-1}$ ($ZnCl_2$-activated biochar). This improvement in the textural properties directly affected the adsorption capacity.

It was also verified that the 2-chlorophenol adsorption increased with the pH decrease. The higher adsorption capacity was obtained at pH 2 for the three biochars investigated, reaching the values of 7.00 mg g^{-1}, 26.68 mg $g^{-1,}$ and 45.00 mg g^{-1} for the non-activated biochar, CO_2-activated biochar and $ZnCl_2$-activated biochar, respectively. In basic pH values, a pronounced decrease of the adsorption capacity was noticed. These observations can be explained considering the ionization aspects of 2-chlorophenol molecules and the surface charge of the biochars. 2-chlorophenol is a week acid (pKa=8.85) and exists as a neutral molecule in acid pH [31]. Similarly, the adsorbent surface becomes highly protonated and positively charged below the pH_{PZC}, which favors the adsorption due to the electrostatic attraction with the 2-chlorophenol neutral molecules [32]. As the pH of the solution increases, the surface of the adsorbent becomes less positively charged, weakening the electrostatic attraction between the adsorbate and the adsorbent, reducing the adsorption capacity. The increase of the pH above the pH_{PZC} makes the biochar surface negatively charged, and when pH>pKa (8.85), 2-chlorophenol molecules start to undergo to an anionic form. Thus, an electrostatic repulsion interaction can take place between the adsorbate and the adsorbent. Furthermore, the competitive adsorption of OH^- ions can also result in a decrease in the adsorption capacity [32].

From the behavior of the adsorption of 2-chlorophenol using $ZnCl_2$-activated biochar in different initial pH values, it is possible to observe that the adsorption capacity remained practically constant in the pH range from 2 to 6. Above pH 8, the adsorption capacity decreases. For the non-activated biochar and CO_2-activated biochar, the adsorption capacity remains constant in the range of pH from 2 to 4 and after begins to decrease. These specificities can be explained since $ZnCl_2$-activated biochar has more hydroxyl groups. Although $ZnCl_2$-activated biochar has net negative charge above pH

3.36, which only occurs at pH 6.28 and 6.42 for the non-activated biochar and CO_2-activated biochar, respectively, the number of positively charged hydroxyl sites can be greater than in the non-activated biochar and CO_2-activated biochar, thus possessing greater electrostatic attraction with the 2-chlorophenol molecules.

Since $ZnCl_2$-activated biochar exhibited the higher adsorption capacities, the subsequent adsorption studies were conducted using this adsorbent. Besides that, the subsequent experiments were carried out at pH 6, where the adsorbent efficiency was suitable.

3.3. Adsorption kinetic profile

The adsorption kinetics express how much of the adsorbate is removed from the liquid phase as a function of time. The kinetic study of 2-chlorophenol adsorption on $ZnCl_2$-activated biochar was carried out at pH 6.0, varying the initial 2-chlorophenol concentration from 25 to 300 mg L^{-1}. Fig 4 shows the results

It can be reported the increase in adsorption capacity with the initial concentration of 2-chlorophenol, as also presented in the literature [33]. Besides, it was possible to evaluate that, regardless of the initial concentration of 2-chlorophenol, adsorption was fast in the first 20 min of the process, reaching its equilibrium in approximately 60 min. This trend occurs because at the beginning of the process, the adsorbent sites are fully available, and these sites are progressively occupied along the time.

The kinetic parameters are shown in Table 2. In Table 2, it is possible to observe that all models used were adequate to describe the kinetic data. However, the pseudo-second-order model stands out since the determination coefficient *(R^2)*, and adjusted

determination coefficient *(R^2_{adj})* were the highest presented and the average relative error *(ARE)* was the lower. In summary, 2-chlorophenol adsorption on $ZnCl_2$-activated biochar followed the pseudo-second-order model. The q_2 values increased with the initial concentration of 2-chlorophenol, agreeing with the experimental behavior. Furthermore, q_2 values closed with the experimental values *(q_e)*. The initial sorption rate parameter *(h_0)* was directly proportional to C_0, indicating that, at the initial stages, 2-chlorophenol was faster adsorbed at higher C_0 values.

3.4. Equilibrium isotherms

Fig. 5 shows the equilibrium isotherm curves of 2-chlorophenol adsorption on $ZnCl_2$-activated biochar at different temperatures. According to Giles et al. [34], the isotherm curves are L1 type. In general, they indicate that the adsorbed molecules present strong intermolecular attractions. The isotherms were favorable, but it is possible to see that the plateau was not reached in the concentration ranges used, which may be an indication that the adsorption sites were not completely occupied [34]. It is also noticeable that the isotherm curves were favored with an increase in temperature. The behavior of isotherms suggests an endothermic adsorption process. This trend is normally attributed to the thermal collision phenomenon.

The isotherm parameters are depicted in Table 3. According to the values of (R^2), (R^2_{adj}), and (*ARE*), the equation that best fits the experimental data was the Freundlich model. This trend suggests that sites with different energies are present on the biochar surface, which was confirmed by the FT-IR spectrum. The Freundlich constant (k_F),

which is associated with the adsorption capacity, increased with the temperature confirming high adsorption capacities at 328 K. Since the Freundlich model has not a specific parameter for adsorption capacity, the experimental value was used for comparison. Here, $ZnCl_2$-activated biochar presented an adsorption capacity of 150 mg g^{-1} for 2-chlorophenol (Fig. 5). This value can be considered adequate and promising for adsorption of the 2-chlorophenol compound, when compared to the literature. The following 2-chlorophenol adsorption capacities have been reported: 25.94 [1], 70.52 [35] and 225 mg g^{-1} [2].

3.5. Thermodynamic results

Freundlich parameters were used to estimate the values of ΔG^0, ΔH^0 and ΔS^0. The thermodynamic parameters are shown in Table 4. The results obtained for ΔG^0 represent that the increase in temperature provides more energy available in the system; the negative value confirms the spontaneity of the process. The positive value obtained for ΔH^0 confirms that the adsorption of 2-chlorophenol on the $ZnCl_2$-activated biochar is an endothermic process. The value of ΔH^0 obtained in this work indicates that the interaction between the adsorbent and adsorbate occurs by physisorption, as it presents energy below 40 kJ mol^{-1} [36]. The positive value of ΔS^0 suggests that there is an increase in structural disorder after the adsorption process.

3.6. Regeneration study

The reuse of the produced adsorbent ($ZnCl_2$-activated biochar) was tested to verify the regeneration capacity. Fig. 6 shows the cycles used to test the adsorption

capacity. The first cycle presented an adsorption capacity of 52.7 mg g^{-1}. This capacity was maintained for five cycles. After the fifth cycle, the capacity decreased to 27.5 mg $g^{-1,}$ and the other cycles showed a drop below 20 mg g^{-1}. This decrease in adsorption capacity after consecutive cycles can be related to the thermal treatment used for desorption. The thermal treatment under the air atmosphere can have destroyed the pores and, consequently, the reduction of porosity and surface area. Furthermore, the adsorption sites were possibly damaged by the temperature. Studies using carbon-based materials to uptake organic compounds from aqueous solutions also reported that your adsorbents could be reused for consecutive cycles. Zazycki et al. [37] prepared a char from MDF wastes to remove a food dye from solutions. They found that the char could be used for 8 adsorption/desorption cycles. Lütke et al. [22] developed an activated carbon from black wattle bark to remove phenol from effluents. They found that the material can be used in two cycles, with a slight decrease in adsorption capacity. In this work, it is suggested the reuse of $ZnCl_2$-activated biochar for 5 times. After 5 cycles, adsorption capacity is not suitable.

3.7. Efficiency in the treatment of simulated effluent

An effluent was prepared to verify the efficiency of $ZnCl_2$-activated biochar to remove several phenolic compounds. The simulated effluent was treated using different dosages of the activated biochar, and the spectra of the simulated effluent before and after the treatments were acquired from 200 to 600 nm using a UV-Vis spectrophotometer. These spectra are shown in Fig. 7. The areas under the absorption bands from 200 and 600 nm were used to measure the amount of phenolic compounds removed from the synthetic effluent. The removal percentages were calculated from the

areas under the absorption bands. At first, it can be seen that the bands in the spectra after the treatment were amortized, indicating that the compounds were removed from the liquid. $ZnCl_2$-activated biochar presented efficiencies of 50.2%, 81.0%, and 98.2% for the effluent treatment, using dosages of 1 g L^{-1}, 5 g $L^{-1,}$ and 10 g L^{-1}, respectively. These results indicate that $ZnCl_2$-activated biochar is an efficient adsorbent for the treatment of industrial effluents containing phenolic compounds.

4. Conclusion

Novel activated biochars were produced from malt bagasse by chemical and physical activations, and were applied in the remediation of effluents containing 2-chlorophenol. The specific surface areas of CO_2 activated biochar, and $ZnCl_2$-activated biochar were 161 m^2 g^{-1} and 545 m^2 g^{-1}, respectively. Therefore, the most efficient activation was with $ZnCl_2$. The CO_2 and $ZnCl_2$ activated biochars were characterized as mesoporous. Both activated biochars exhibited an amorphous structure and the presence of hydroxyl functional groups. $ZnCl_2$-activated biochar presented more cavities on the surface when compared with CO_2 activated biochar.

The adsorption of 2-chlorophenol on the biochars was favored under acid conditions. $ZnCl_2$-activated biochar was more efficient in removing 2-chlorophenol from aqueous solutions than CO_2 activated biochar. 2-chlorophenol adsorption on $ZnCl_2$-activated biochar followed the pseudo-second order model, being the equilibrium attained within 60 min. Freundlich model showed a better fit with the isotherm curves. The maximum adsorption capacity was 150 mg g^{-1}. Adsorption process was endothermic and spontaneous. The reuse of $ZnCl_2$-activated biochar can be performed by 5 times. $ZnCl_2$-activated biochar is an excellent adsorbent to polish industrial

effluents containing phenolic compounds and salts, with an efficiency of 98.21% (using a dosage of 10 g L^{-1}).

Author Contribution Statement

L.M.M. Machado: Conceptualization, Investigation, Resources, Original Draft.

S.F. Lütke: Methodology, Resources, Original Draft.

D. Perondi: Conceptualization, Methodology, Formal analysis, Original Draft, Visualization.

M. Godinho: Supervision, Project administration, Funding acquisition, Conceptualization, Review & Editing.

M. L. S. Oliveira: Conceptualization, Review & Editing.

G.C. Collazzo: Conceptualization, Methodology.

G.L. Dotto: Supervision, Project administration, Funding acquisition, Conceptualization, Review & Editing.

Declaration of interests

The authors declare that they have no known competing financial interests or personal relationships that could have appeared to influence the work reported in this paper.

References

[1] A. Adewuyi, A. Göpfert, O. Anuoluwapo, T. Wolff, Adsorption of 2-chlorophenol onto the surface of underutilized seed of Adenopus brevi florus : A

potential means of treating waste water, J. Environ. Chem. Eng. 4 (2016) 664–672. doi:10.1016/j.jece.2015.12.012.

[2] T.K.M. Prashanthakumar, S.K.A. Kumar, S.K. Sahoo, A quick removal of toxic phenolic compounds using porous carbon prepared from renewable biomass coconut spathe and exploration of new source for porous carbon materials, J. Environ. Chem. Eng. 6 (2018) 1434–1442. doi:10.1016/j.jece.2018.01.051.

[3] Ç. Kırbıyık, A.E. Pütün, E. Pütün, Equilibrium, kinetic, and thermodynamic studies of the adsorption of Fe(III) metal ions and 2,4-dichlorophenoxyacetic acid onto biomass-based activated carbon by ZnCl2 activation, Surfaces and Interfaces. 8 (2017) 182–192. doi:10.1016/j.surfin.2017.03.011.

[4] N. Taoufik, A. Elmchaouri, F. Anouar, S.A. Korili, A. Gil, Improvement of the adsorption properties of an activated carbon coated by titanium dioxide for the removal of emerging contaminants, J. Water Process Eng. 31 (2019) 100876. doi:10.1016/j.jwpe.2019.100876.

[5] N.B. Singh, G. Nagpal, S. Agrawal, Rachna, Water purification by using Adsorbents: A Review, Environ. Technol. Innov. 11 (2018) 187–240. doi:10.1016/j.eti.2018.05.006.

[6] Z.N. Garba, W. Zhou, I. Lawan, W. Xiao, M. Zhang, L. Wang, L. Chen, Z. Yuan, An overview of chlorophenols as contaminants and their removal from wastewater by adsorption: A review, J. Environ. Manage. 241 (2019) 59–75. doi:10.1016/j.jenvman.2019.04.004.

[7] G.L. Dotto, G. McKay, Current scenario and challenges in adsorption for water treatment, J. Environ. Chem. Eng. 8 (2020) 103988. doi:10.1016/j.jece.2020.103988.

[8] P.S. Thue, M.A. Adebayo, E.C. Lima, J.M. Sieliechi, F.M. Machado, G.L. Dotto,

J.C.P. Vaghetti, S.L.P. Dias, Preparation , characterization and application of microwave-assisted activated carbons from wood chips for removal of phenol from aqueous solution, J. Mol. Liq. 223 (2016) 1067–1080. doi:10.1016/j.molliq.2016.09.032.

[9] M.A. Zazycki, M. Godinho, D. Perondi, E.L. Foletto, G.C. Collazzo, G.L. Dotto, New biochar from pecan nutshells as an alternative adsorbent for removing reactive red 141 from aqueous solutions, J. Clean. Prod. 171 (2018) 57–65. doi:10.1016/j.jclepro.2017.10.007.

[10] K.M. Lynch, E.J. Steffen, E.K. Arendt, Brewers ' spent grain : a review with an emphasis on food and health, (2016). doi:10.1002/jib.363.

[11] M.A. Franciski, E.C. Peres, M. Godinho, D. Perondi, E.L. Foletto, G.C. Collazzo, G.L. Dotto, Development of CO2 activated biochar from solid wastes of a beer industry and its application for methylene blue adsorption, Waste Manag. 78 (2018) 630–638. doi:10.1016/j.wasman.2018.06.040.

[12] A.M. Carvajal-Bernal, F. Gómez, L. Giraldo, J.C. Moreno-Piraján, Adsorption of phenol and 2,4-dinitrophenol on activated carbons with surface modifications, Microporous Mesoporous Mater. 209 (2015) 150–156. doi:10.1016/j.micromeso.2015.01.052.

[13] M.A. Yahya, Z. Al-Qodah, C.W.Z. Ngah, Agricultural bio-waste materials as potential sustainable precursors used for activated carbon production: A review, Renew. Sustain. Energy Rev. 46 (2015) 218–235. doi:10.1016/j.rser.2015.02.051.

[14] J.N. Sahu, J. Acharya, B.C. Meikap, Optimization of production conditions for activated carbons from Tamarind wood by zinc chloride using response surface methodology, Bioresour. Technol. 101 (2010) 1974–1982. doi:10.1016/j.biortech.2009.10.031.

[15] L. Duan, Q. Ma, L. Ma, L. Dong, B. Wang, X. Dai, B. Zhang, Effect of the CO2 activation parameters on the pore structure of silicon carbide-derived carbons, New Carbon Mater. 34 (2019) 367–372. doi:10.1016/s1872-5805(19)30022-8.

[16] L.M.M. Machado, S.F. Lütke, D. Perondi, M. Godinho, M.L.S. Oliveira, G.C. Collazzo, G.L. Dotto, Simultaneous production of mesoporous biochar and palmitic acid by pyrolysis of brewing industry wastes, Waste Manag. 113 (2020) 96–104. doi:10.1016/j.wasman.2020.05.038.

[17] A.F.M. Streit, L.N. Côrtes, S.P. Druzian, M. Godinho, G.C. Collazzo, D. Perondi, G.L. Dotto, Development of high quality activated carbon from biological sludge and its application for dyes removal from aqueous solutions, Sci. Total Environ. 660 (2019) 277–287. doi:10.1016/j.scitotenv.2019.01.027.

[18] Y.S. Ho, G.M.F.E. Llow, Kinetic M Odels for Th E Sorption O F Dye Fro M Aqueous Solution By W O Od, Trans IChemE. 76 (1998) 183–191.

[19] I. Langmuir, The adsorption of gases on plane surfaces of glass, mica and platinum, J. Am. Chem. Soc. 40 (1918) 1361–1403. doi:10.1021/ja02242a004.

[20] Z.Y. Yao, J.H. Qi, L.H. Wang, Equilibrium, kinetic and thermodynamic studies on the biosorption of Cu(II) onto chestnut shell, J. Hazard. Mater. 174 (2010) 137–143. doi:10.1016/j.jhazmat.2009.09.027.

[21] P.S. Thue, G.S. Reis, Activated carbon obtained from sapelli wood sawdust by microwave heating for o -cresol adsorption, Res. Chem. Intermed. 43 (2017) 1063–1087. doi:10.1007/s11164-016-2683-8.

[22] S.F. Lütke, A. V Igansi, L. Pegoraro, G.L. Dotto, L.A.A. Pinto, T.R.S. Cadaval, Journal of Environmental Chemical Engineering Preparation of activated carbon from black wattle bark waste and its application for phenol adsorption, J. Environ. Chem. Eng. 7 (2019) 103396. doi:10.1016/j.jece.2019.103396.

[23] M. Thommes, K. Kaneko, A. V. Neimark, J.P. Olivier, F. Rodriguez-Reinoso, J. Rouquerol, K.S.W. Sing, Physisorption of gases, with special reference to the evaluation of surface area and pore size distribution (IUPAC Technical Report), Pure Appl. Chem. 87 (2015). doi:10.1515/pac-2014-1117.

[24] K.B. Fontana, E.S. Chaves, J.D.S. Sanchez, E.R.L.R. Watanabe, J.M.T.A. Pietrobelli, G.G. Lenzi, Textile dye removal from aqueous solutions by malt bagasse: Isotherm, kinetic and thermodynamic studies, Ecotoxicol. Environ. Saf. 124 (2016) 329–336. doi:10.1016/j.ecoenv.2015.11.012.

[25] M.A. Yahya, Z. Al-Qodah, C.W.Z. Ngah, Agricultural bio-waste materials as potential sustainable precursors used for activated carbon production: A review, Renew. Sustain. Energy Rev. 46 (2015) 218–235. doi:10.1016/j.rser.2015.02.051.

[26] N. Mohamad Nor, L.C. Lau, K.T. Lee, A.R. Mohamed, Synthesis of activated carbon from lignocellulosic biomass and its applications in air pollution control - A review, J. Environ. Chem. Eng. 1 (2013) 658–666. doi:10.1016/j.jece.2013.09.017.

[27] C. Herrero-Latorre, J. Barciela-García, S. García-Martín, R.M. Peña-Crecente, Graphene and carbon nanotubes as solid phase extraction sorbents for the speciation of chromium: A review, Anal. Chim. Acta. 1002 (2018) 1–17. doi:10.1016/j.aca.2017.11.042.

[28] Y. Sun, Q. Yue, Y. Mao, B. Gao, Y. Gao, L. Huang, Enhanced adsorption of chromium onto activated carbon by microwave-assisted H3PO4 mixed with Fe/Al/Mn activation, J. Hazard. Mater. 265 (2014) 191–200. doi:10.1016/j.jhazmat.2013.11.057.

[29] R. Labied, O. Benturki, A.Y. Eddine Hamitouche, A. Donnot, Adsorption of hexavalent chromium by activated carbon obtained from a waste lignocellulosic

material (Ziziphus jujuba cores): Kinetic, equilibrium, and thermodynamic study, Adsorpt. Sci. Technol. 36 (2018) 1066–1099. doi:10.1177/0263617417750739.

[30] W. Liu, J. Zhang, C. Zhang, Y. Wang, Y. Li, Adsorptive removal of Cr (VI) by Fe-modified activated carbon prepared from Trapa natans husk, Chem. Eng. J. 162 (2010) 677–684. doi:10.1016/j.cej.2010.06.020.

[31] T. Soltani, B.K. Lee, Mechanism of highly efficient adsorption of 2-chlorophenol onto ultrasonic graphene materials: Comparison and equilibrium, J. Colloid Interface Sci. 481 (2016) 168–180. doi:10.1016/j.jcis.2016.07.049.

[32] L. Zhang, B. Zhang, T. Wu, D. Sun, Y. Li, Adsorption behavior and mechanism of chlorophenols onto organoclays in aqueous solution, Colloids Surfaces A Physicochem. Eng. Asp. 484 (2015) 118–129. doi:10.1016/j.colsurfa.2015.07.055.

[33] M. Foroughi-Dahr, H. Abolghasemi, M. Esmaili, A. Shojamoradi, H. Fatoorehchi, Adsorption Characteristics of Congo Red from Aqueous Solution onto Tea Waste, Chem. Eng. Commun. 202 (2015) 181–193. doi:10.1080/00986445.2013.836633.

[34] C.H. Giles, T.H. MacEwan, S.N. Nakhwa, D. Smith, **S**tudies in adsorption. Part XI. A system of classification of solution adsorption isotherms, and its use in diagnosis of adsorption mechanisms and in measurement of specific surface areas of solids, J. Chem. Soc. 786 (1960) 3973.

[35] L.C. Zhou, X.G. Meng, J.W. Fu, Y.C. Yang, P. Yang, C. Mi, Highly efficient adsorption of chlorophenols onto chemically modified chitosan, Appl. Surf. Sci. 292 (2014) 735–741. doi:10.1016/j.apsusc.2013.12.041.

[36] A. Bonilla-Petriciolet, D.I. Mendoza-Castillo, H.E. Reynel-Ávila, Adsorption Processes for Water Treatment and Purification, 2017. doi:10.1016/S0301-

7036(14)70853-3.

[37] M.A. Zazycki, D. Perondi, M. Godinho, M.L.S. Oliveira, G.C.Collazzo, G.L.Dotto, Conversion of MDF wastes into a char with remarkable potential to remove Food Red 17 dye from aqueous effluents, Chemosphere 250 (2020) 126248. doi: 10.1016/j.chemosphere.2020.126248.

Figure captions

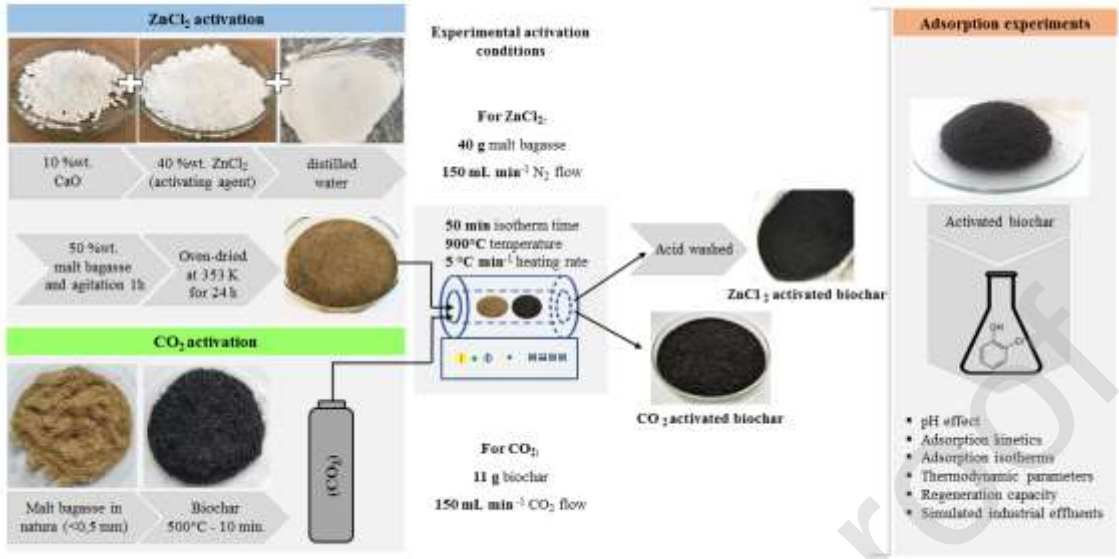

Fig. 1. Procedure for biochar activation ($ZnCl_2$ and CO_2) and adsorption process.

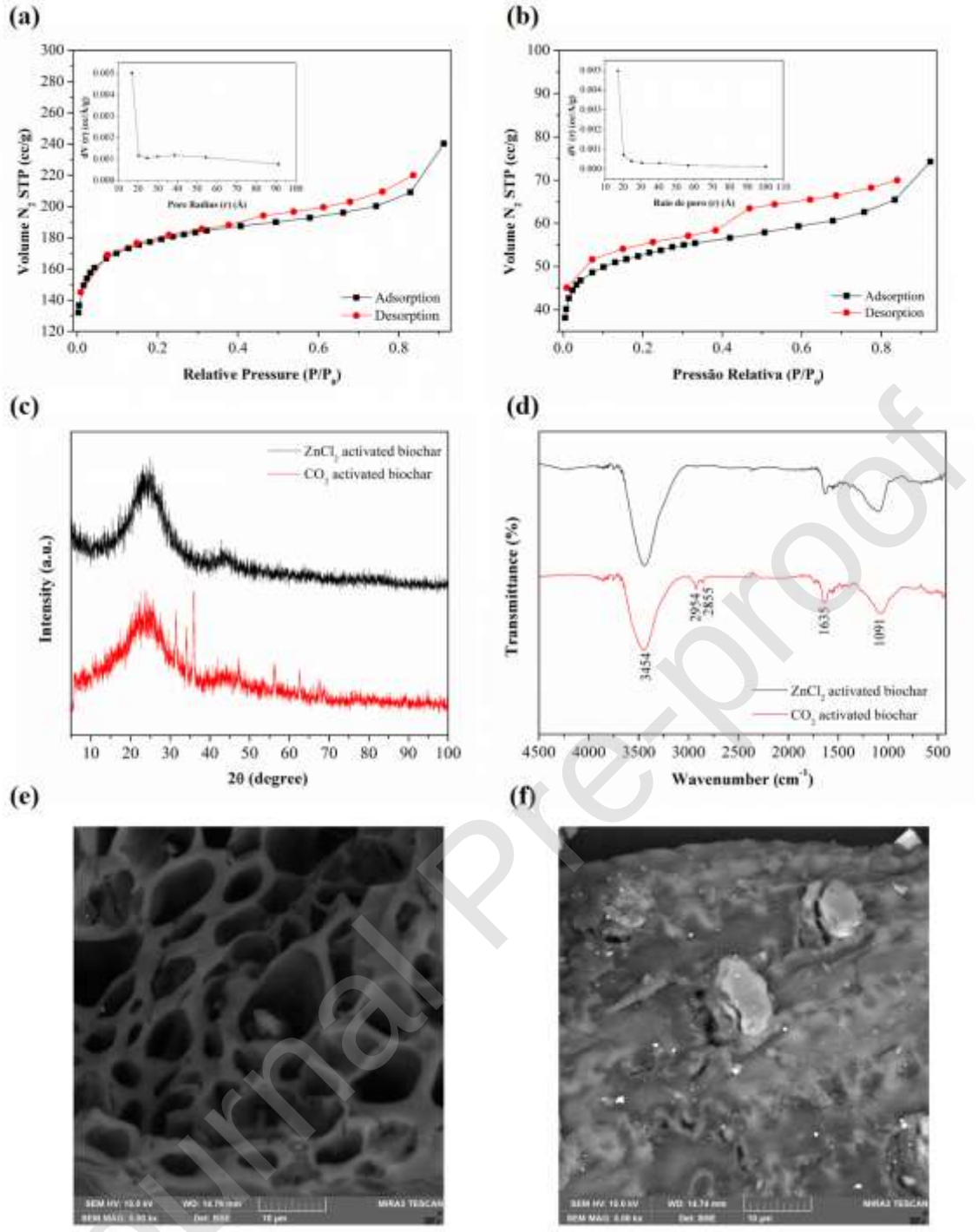

Fig. 2. Characterization of activated biochars: BET/BJH. (a) $ZnCl_2$-activated biochar and (b) CO_2-activated biochar; (c) XRD; (d) FTIR; (e) $ZnCl_2$-activated biochar SEM and (f) CO_2-activated biochar SEM.

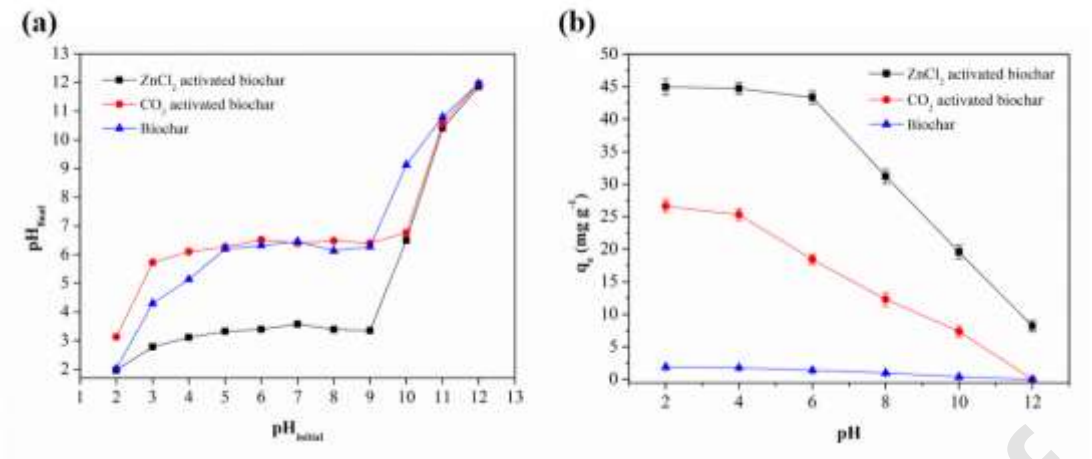

Fig. 3. pH_{PZC} (a) and pH effect on 2-chlorophenol adsorption (b).

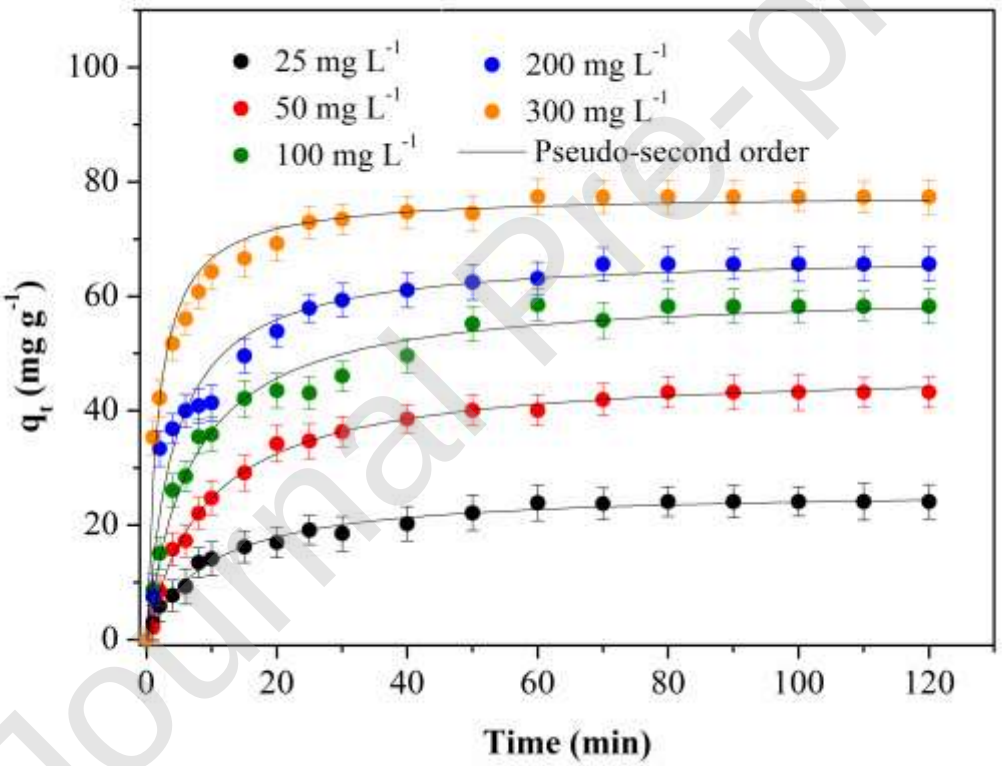

Fig. 4. Kinetic curves of 2-chlorophenol adsorption on $ZnCl_2$-activated biochar (298 K, pH = 6.0).

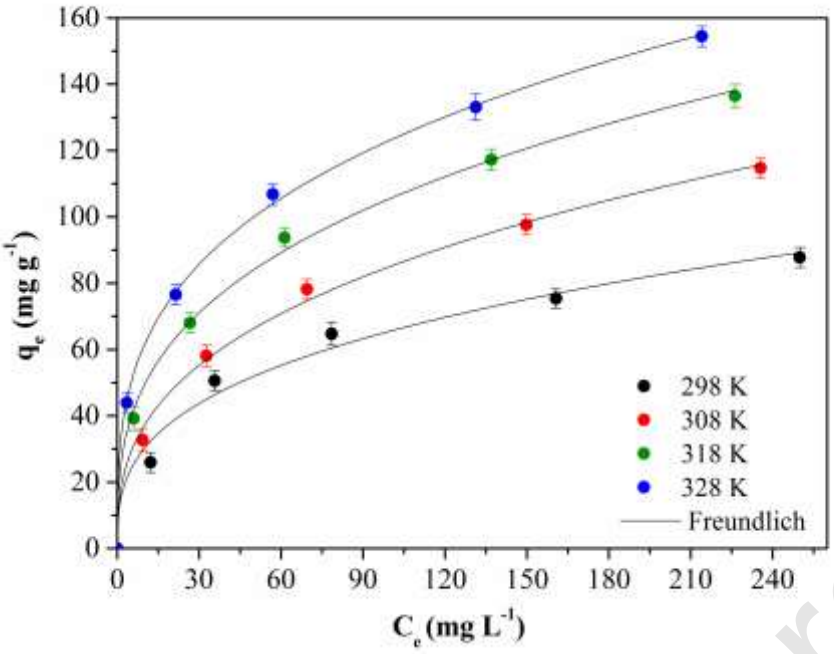

Fig. 5. Equilibrium isotherm curves of 2-chlorophenol adsorption on $ZnCl_2$-activated biochar (pH = 6.0).

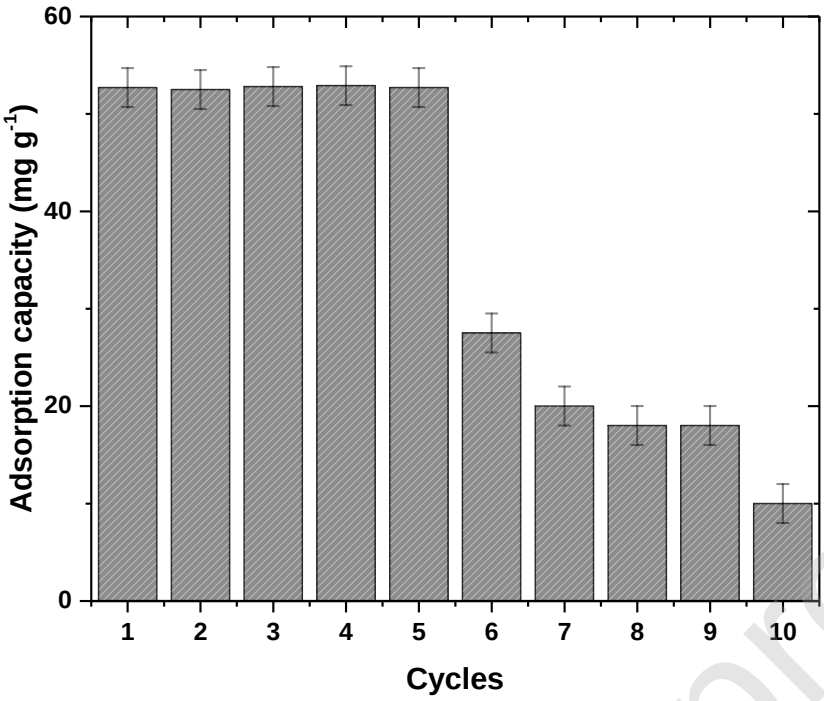

Fig. 6. Adsorption capacity of $ZnCl_2$-activated biochar after consecutive adsorption/desorption cycles.

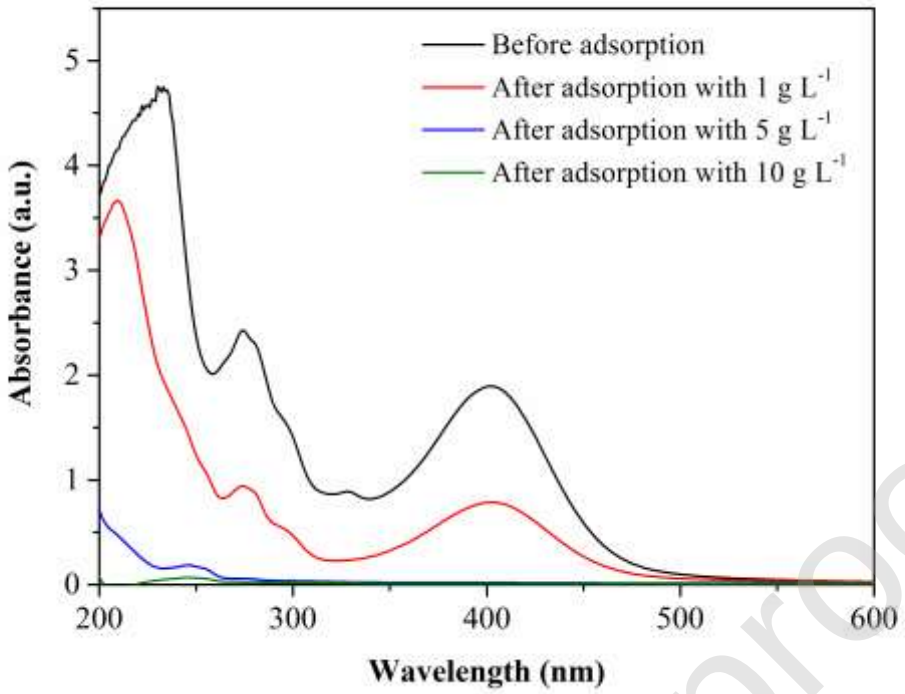

Fig. 7. Visible spectra of simulated effluent before and after adsorption using $ZnCl_2$-activated biochar.

Table captions

Table 1. Simulated effluent composition.

	Concentration (mg L^{-1})
Phenols	
2-Chlorophenol	60
Phenol	10
Bisphenol A	10
2-Nitrophenol	10
4-Nitrophenol	10
2-Naphthol	10
Resorcinol	10
Hydroquinone	10
Inorganic compounds	
Sodium sulfate	40
Sodium carbonate	40
Sodium chloride	50
Sodium phosphate	40

Table 2. Kinetic parameters for 2-chlorophenol adsorption on $ZnCl_2$-activated biochar.

	Initial 2-chlorophenol concentration (mg L^{-1})				
Models	**25**	**50**	**100**	**200**	**300**
Pseudo-first order					
q_1 (mg g^{-1})	23.67	43.11	55.05	63.13	75.35
k_1 (min^{-1})	0.0857	0.0835	0.1125	0.1504	0.3216
R^2	0.9699	0.9938	0.9463	0.9163	0.9453
R^2_{adj}	0.9679	0.9932	0.9429	0.9103	0.9407
ARE (%)	9.80	8.84	10.68	10.58	6.59
Pseudo-second order					
q_2 (mg g^{-1})	26.28	47.43	61.23	67.46	77.87
k_2 (g mg^{-1} min^{-1})	0.0041	0.0023	0.0024	0.0036	0.0076
h_0 (mg g^{-1} min^{-1})	2.83	5.17	8.99	16.38	46.08
R^2	0.9900	0.9847	0.9793	0.9622	0.9867
R^2_{adj}	0.9893	0.9830	0.9780	0.9595	0.9865
ARE (%)	5.52	13.57	4.79	10.11	3.33
Avrami					
q_{av} (mg g^{-1})	23.37	43.11	55.06	63.13	75.36
k_{av} (min^{-1})	0.1436	0.2715	0.3235	0.4008	0.5894
n_{av}	0.5967	0.3078	0.3477	0.3753	0.5457
R^2	0.9699	0.9939	0.9463	0.9163	0.9453
R^2_{adj}	0.9679	0.9932	0.9429	0.9407	0.9103
ARE (%)	9.80	8.84	10.68	10.58	6.59
q_e (exp) (mg g^{-1})	24.12	43.25	58.28	65.62	77.35

Table 3. Equilibrium isotherms parameters for 2-chlorophenol adsorption onto $ZnCl_2$ activated biochar.

	Temperature (K)			
Models	**298**	**308**	**318**	**328**
Langmuir				
q_m (mg g^{-1})	95.52	126.24	145.03	157.59
k_L (L mg^{-1})	0.0294	0.0271	0.0362	0.0496
R^2	0.9939	0.9869	0.9777	0.9607
R^2_{adj}	0.9924	0.9836	0.9722	0.9509
ARE (%)	2.92	6.42	8.87	11.82
Freundlich				
k_F ((mg g^{-1})(L mg^{-1})$^{-1/n}$)	13.93	16.30	23.18	30.74
1/nf	0.3363	0.3589	0.3292	0.3015
R^2	0.9848	0.9969	0.9981	0.9994
R^2_{adj}	0.9810	0.9961	0.9976	0.9992
ARE (%)	7.21	3.20	2.14	1.16

Table 4. Thermodynamic parameters estimated for the adsorption of 2-chlorophenol onto $ZnCl_2$-activated biochar.

T **(K)**	ΔG^0 **(kJ mol^{-1})**	ΔH^0 **(kJ mol^{-1})**	ΔS^0 **(kJ K^{-1} mol^{-1})**
298	-5.03	21.08	0.09
308	-5.66		
318	-6.70		
328	-7.61		